NANO LETTERS

2004
Vol. 4, No. 3
391−397

DNA-Directed Synthesis of Generation 7 and 5 PAMAM Dendrimer Nanoclusters

Youngseon Choi,[†,‡] Almut Mecke,[‡,§] Bradford G. Orr,[‡,§] Mark M. Banaszak Holl,[‡,||] and James R. Baker, Jr.*[,†,‡]

Department of Biomedical Engineering, School of Engineering, Department of Physics, School of Literature, Art and Science, and Department of Chemistry, School of Literature, Art and Science, University of Michigan, Ann Arbor, Michigan 48109, and Center for Biologic Nanotechnology, Department of Internal Medicine, University of Michigan Medical School, Ann Arbor, Michigan 48109-0648

Received May 27, 2003; Revised Manuscript Received January 22, 2004

ABSTRACT

A novel nanostructure was constructed using two different generations of polyamidoamine (PAMAM) dendrimers and three sets of complementary oligonucleotides (34, 50, and 66 bases in length). The oligonucleotides were covalently conjugated to partially acetylated generation 5 and 7 PAMAM dendrimers, and these conjugates were characterized by agarose gel electrophoresis. The agarose gel electrophoresis appearance of these covalently linked oligonucleotide dendrimers was also compared to electrostatically bound oligonucleotide−dendrimer complexes. Equimolar amounts of the G5 and G7 conjugates were then hybridized together to allow for the DNA-directed self-assembly of supramolecular clusters. Dynamic light scattering (DLS) analysis indicated that the overall size of the DNA-linked dendrimer clusters tended to increase according to the length of the oligonucleotide used ranging from 30 to 50 nm, which agreed with the diameter of dendrimer nanoclusters predicted by molecular modeling. The DNA-linked novel dendrimer nanoclusters were also examined with tapping-mode atomic force microscopy (AFM) to distinguish the DNA-linked structure from a nonlinked simple G7/G5 dendrimer mixture. AFM image analysis suggested that the distance between the DNA-linked dendrimers was significantly larger than what was seen after simple mixing of G7/G5 dendrimers. The mixture showed a few dendrimers physically in contact with an interdendrimer distance of 8–10 nm. The interdendrimer distance of the nanoclusters linked with the 50-base-long oligonucleotide pairs was measured to be 21 ± 2 nm, which is in agreement with the theoretical length of the oligonucleotides duplex. These results suggest that PAMAM dendrimers can be self-assembled via complementary oligonucleotides to form supramolecular nanoclusters.

The development of 3D assemblies of nanoscale molecules with controlled sizes and shapes is a great challenge for materials chemistry and nanotechnology.[1] Because of their precisely controlled mass, surface valency, and surface functionality, PAMAM dendrimers have been employed as molecular components of unique, mathematically defined nanoscale dendrimer clusters.[2−4] In these elegant structures, charge interaction was employed as a basis for forming covalent bonds to link the components. However, this approach makes the development of complex molecular arrays technically difficult because specific size ratios and covalent chemistry are necessary to coordinate the self-assembly of core and shell dendrimers. There is also no specificity for the coupling of dendrimers so that it is difficult to assemble specific molecules. Thus, alternative approaches to assembling dendrimers into supramolecular clusters need to be developed.

Synthetic oligonucleotides have been widely used as a tool to self-assemble nanoscale objects in precise structural arrangements due to the base specificity of the resulting duplex structure. Since the development of the self-assembly of nanocrystals using DNA by Alivisatos et al.,[5] others have attached oligonucleotides to gold nanoparticles to direct the formation of periodic nanostructures, which can be reversibly assembled.[6,7] In contrast, although charge-based PAMAM−oligonucleotide complexes have been employed for the delivery of antisense oligonucleotides and gene transfection in vitro, no one has used covalently bound PAMAM−oligonucleotide conjugates as a means for generating specific supramolecular clusters.[8−11]

In this study, we attempted to link dendrimers specifically using complementary DNA strands. These clusters were then examined on the nanometer scale by AFM to evaluate the interdendrimer distance in the cluster and document the assembly of different components.

An initial challenge involved linking the negatively charged oligonucleotide to the positively charged amine-terminated PAMAM dendrimers. Although the nature of the electrostatic interaction may enhance the rate of covalent

* Corresponding author. E-mail: jbakerjr@umich.edu.
† Department of Biomedical Engineering.
‡ Center for Biological Nanotechnology.
§ Department of Physics.
|| Chemistry Department.

10.1021/nl0343497 CCC: $27.50
Published on Web 02/21/2004

Table 1. Molecular Properties of Amine-Terminated and Partially Acetylated PAMAM Dendrimers Used for Oligonucleotide Conjugation

samples	no. of terminal NH_2 groups[a]	M_w[a,b] (g/mol)	poly-dispersity index[b]	hydro-dynamic diameter (nm)[b]
G7	434 (512)	111 600 (116 493)	1.068	5.4
G7-Ac89	48	114 800	1.031	5.0
G5	120 (128)	25 920 (28 826)	1.045	5.0
G5-Ac90	12	31 600	1.017	4.7

[a] Determined by using potentiometric titration; dendrimer (10 mg) dissolved in 0.1 N NaCl solution was first fully protonated by the addition of a 0.1 N HCl standard solution, followed by titrating with a 0.1 N NaOH standard solution at 3-min time intervals using a Corning 420 pH meter with a Corning glass combination electrode at 20 °C. Numbers in parentheses are theoretical values. [b] Data from a size-exclusion chromatography system consisting of a Waters 510 HPLC pump, a TSK precolumn followed by three analytical columns (G4000PW, G3000PW, and G2000PW), and a Wyatt Refracting Index dual detector at 25 °C (run time, 60 min). The mobile phase was 0.1 M citric acid/0.025% NaN_3 in H_2O. Molecular weights and M_w distributions as the polydispersity index were obtained by assuming 100% recovery using Astramol software 2.0 (Millipore Co.).

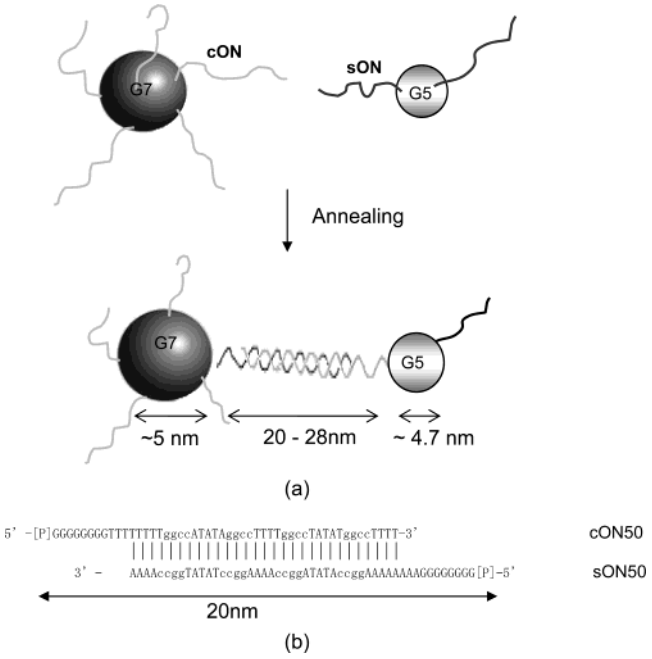

Figure 1. (a) Schematic of the self-assembly of G7 and G5 PAMAM dendrimers using 5′-phosphate-modified oligonucleotides (cON and sON; 34, 50, or 66 bases), which are partially complementary in their sequences. The diameter of a dendrimer is based on the hydrodynamic radius obtained from SEC, as shown in Table 1. (b) Example of partial complementary base pairs, which are in their most favorable state between cON and sON in terms of interaction free energies ($\Delta G = -71.6$ kcal/mol at 25 °C) calculated from Vector NTI software. [P] represents a phosphate group.

bond formation,[12] minimizing the electrostatic association to a certain extent is necessary for the prevention of infinite network formation.[13] Thus, we controlled the surface charge density of the primary amines of the dendrimers by substituting with a certain number of acetyl groups. Recent studies indicated that the acetylation of PAMAM dendrimer surface amines is controllable and prevents the nonspecific interaction of the polymer with cells.[14,15] We also expected that

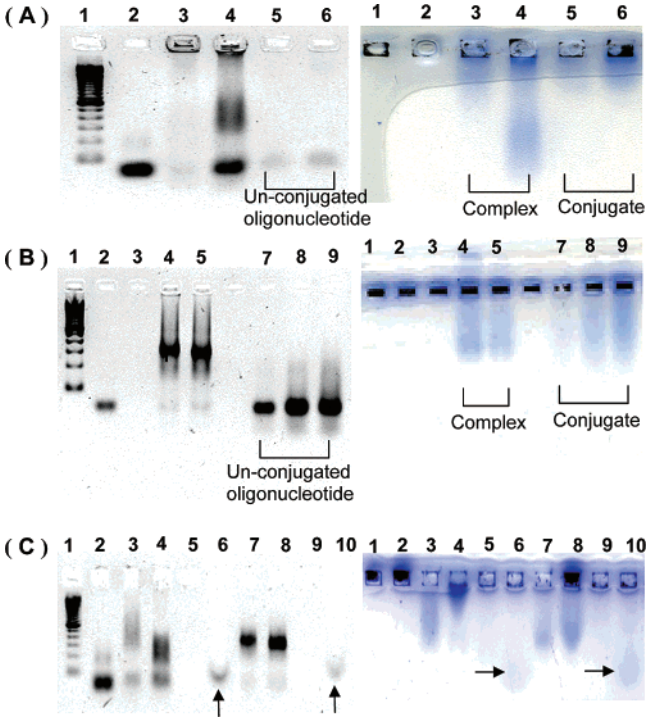

Figure 2. Agarose gel electrophoresis characterization of oligonucleotide (66- mer)-conjugated G7 and G5 PAMAM dendrimers. The left panels of the gels are stained with EtBr for the oligonucleotide, and the right panels, with colloidal blue, which stains the dendrimer. (A) Identification of the G7-cON66 conjugate and the unreacted oligonucleotide; lane 1, 100 bp ladder (0.1 μg); lane 2, 66-mer oligonucleotide (cON66, 0.1 μg); lane 3, G7-Ac89 (10 μg) + cON66 (1 μg) 1:1 molar complex; lane 4, G7-Ac89 (10 μg) + cON66 (2 μg) 1:2 molar complex; lane 5, G7-Ac-cON66 conjugate (3 μL) before gel purification; lane 6, G7-Ac-cON66 conjugate (7 μL) before gel purification. (B) Identification of G5-sON66 conjugate and the unreacted oligonucleotide; lane 1, 100 bp ladder (0.1 μg); lane 2, 66-mer oligonucleotide (sON66, 0.05 μg); lane 4, 1:1 molar complex (G5-Ac/sON66); lane 5, 1:2 molar complex (G5-Ac90/sON66); lanes 7−9, G5-Ac-sON66 conjugate (1, 3, and 6 μL). In the case of the 34-mer and 50-mer conjugation, the migration patterns of the conjugates were the same with this figure. (C) SDS treatment on the conjugates; lane 1, 100 bp ladder (0.1 μg); lane 2, 66-mer oligonucleotide (cON66, 0.1 μg); lane 3, G7-cON66 1:2 molar complex; lane 4, G7-cON66 1:2 molar complex with 1 wt (w/v)% SDS; lane 5, G7-cON66 1:2 molar conjugate after gel purification; lane 6, G7-Ac-cON66 1:2 molar conjugate with SDS; lane 7, G5-sON66 1:2 molar complex; lane 8, G5-sON66 1:2 molar complex with 1 wt (w/v)% SDS; lane 9, G5-sON66 1:2 molar conjugate after gel purification; lane 10, G5-sON66 1:2 molar conjugate with SDS.

limiting the number of available surface primary amines would help to control the number of oligonucleotides attached to each dendrimer. However, considering the densely packed dendrimer surface structure and the potential difficulty of oligonucleotide strand access to dendrimer surface primary amines, the acetylation was limited to 90% of the amines so that on average 12 amine groups per G5 dendrimer and 108 amine groups per G7 dendrimer would remain available for oligonucleotide conjugation. The molecular characteristics of each of the acetylated dendrimers are summarized in Table 1.

To the partially acetylated G7 and G5 PAMAM dendrimers (5 to 7 nm in mean diameter[16]), partially complementary

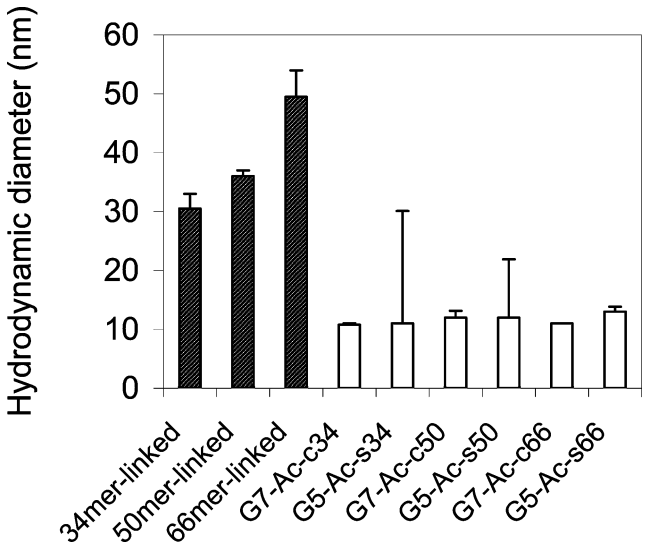

Figure 3. Dynamic light scattering measurement of dendrimer−oligonucleotide conjugates and their DNA-linked dendrimer clusters. The diameter of the dendrimer alone was found to be below the detection limit of the measurement (less than 10 nm). The diameter is obtained from a number-weighted NICOMP distribution analysis where no prior assumption of the shape of the final distribution is made and a nonlinear least-squares method (i.e., an inverse Laplace transform algorithm) is employed. The value was the average of three measurements.

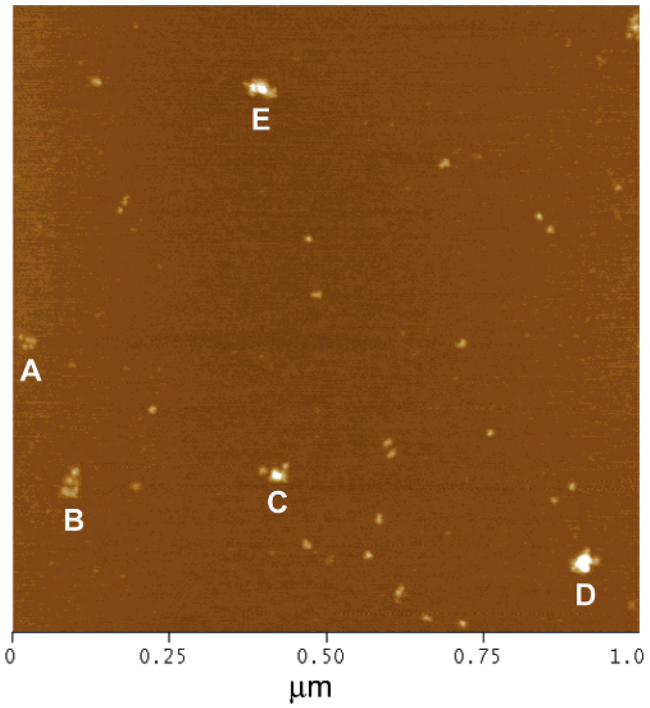

Figure 4. Representative AFM image of a mixture of the G7 and G5 PAMAM dendrimers (7nM) (1:1 molar ratio of G7-Ac89/G5-Ac90).

oligonucleotides (5′-phosphate-modified; 34, 50, and 66 bases in length) were covalently attached using EDC/imidazole chemistry.[17] The sequence of the oligonucleotides was designed to have the first 16 or 32 nucleotides serve as a "spacer" from the dendrimer and the final 34 nucleotides to be available for complementary base pairing. To prevent precipitate formation caused by charge neutralization, an excess of either positively charged dendrimer or negatively charged oligonucleotide was used in the absence or presence of LiCl.[18] LiCl is known to weaken electrostatic interactions between oppositely charged polymers.[19] Briefly, 1−5 equiv of an oligonucleotide/dendrimer molar concentration was activated with 1-ethyl-3-3-dimethylaminopropyl carbodiimide hydrochloride (EDC, Aldrich) in 0.1 M imidazole (pH 6.0) for 10 min at room temperature. The activated oligonucleotide was slowly added to a solution of the partially acetylated PAMAM dendrimer in the presence or absence of 0.5 M LiCl. The mixture was then allowed to react overnight at room temperature. Small molecules such as the isourea byproduct and salts were removed using a membrane filter device (Centricon, YM-10). The nonconjugated oligonucleotide was purified from the oligonucleotide−dendrimer conjugate using preparative agarose gel electrophoresis (1% low-melting agarose, 1x tris−borate−EDTA buffer).

To confirm the covalent bond formation between the dendrimer and the oligonucleotide via the phosphoramidate bond, analytical agarose gel electrophoresis was employed and compared to the electrostatic dendrimer−oligonucleotide complex (Figure 2). The migration pattern of the oligonucleotide−conjugated dendrimer was found to be significantly different from that of the corresponding oligonucleotide−dendrimer complex prepared at the same molar ratio. Once the oligonucleotides were covalently attached to the dendrimer, the resulting conjugate became negatively charged as compared to the partially acetylated dendrimers that retain a slight positive charge at the buffer conditions in the gel (pH 8.0). This implies that a significant number of oligonucleotides are present on the dendrimer. For the partially acetylated G7 dendrimer that has 108 (+) charges, it was concluded that at least two 66-base-long oligonucleotide (cON66) would be attached to the surface of the dendrimer; for the partially acetylated G5 dendrimer that has 16 (+) charges, at least one 66-base-long oligonucleotide (sON66) should be covalently linked to the dendrimer. Unreacted oligonucleotides left in the conjugation mixture migrated in the gel as free oligonucleotide. In the presence of 1 wt % (w/v) sodium dodecyl sulfate (SDS), which disrupts DNA/dendrimer complexes,[20] the oligonucleotide in the conjugate was not dissociated but rather migrated together with the dendrimer (Figure 2c). This electrophoretic analysis documented that the oligonucleotide was in fact coupled to the dendrimer with a stable covalent linkage. Interestingly, the presence of SDS in the conjugate increased the electrophoretic mobility of the conjugate when compared with that of the complex. This might be attributed to the increased negative charge of the oligonucleotide-conjugated dendrimer because a few strands of the 66-mer oligonucleotide were covalently attached to the dendrimer. Some free G5 dendrimer that did not complex with the oligonucleotide was also identified in lane 4 of the right panel of Figure 2b as it migrated in the opposite direction. This suggests that the negatively charged oligonucleotides complex with the dendrimers on a charge basis, resulting in a complex without specific stoichiometry.[21] However, the covalent linking of

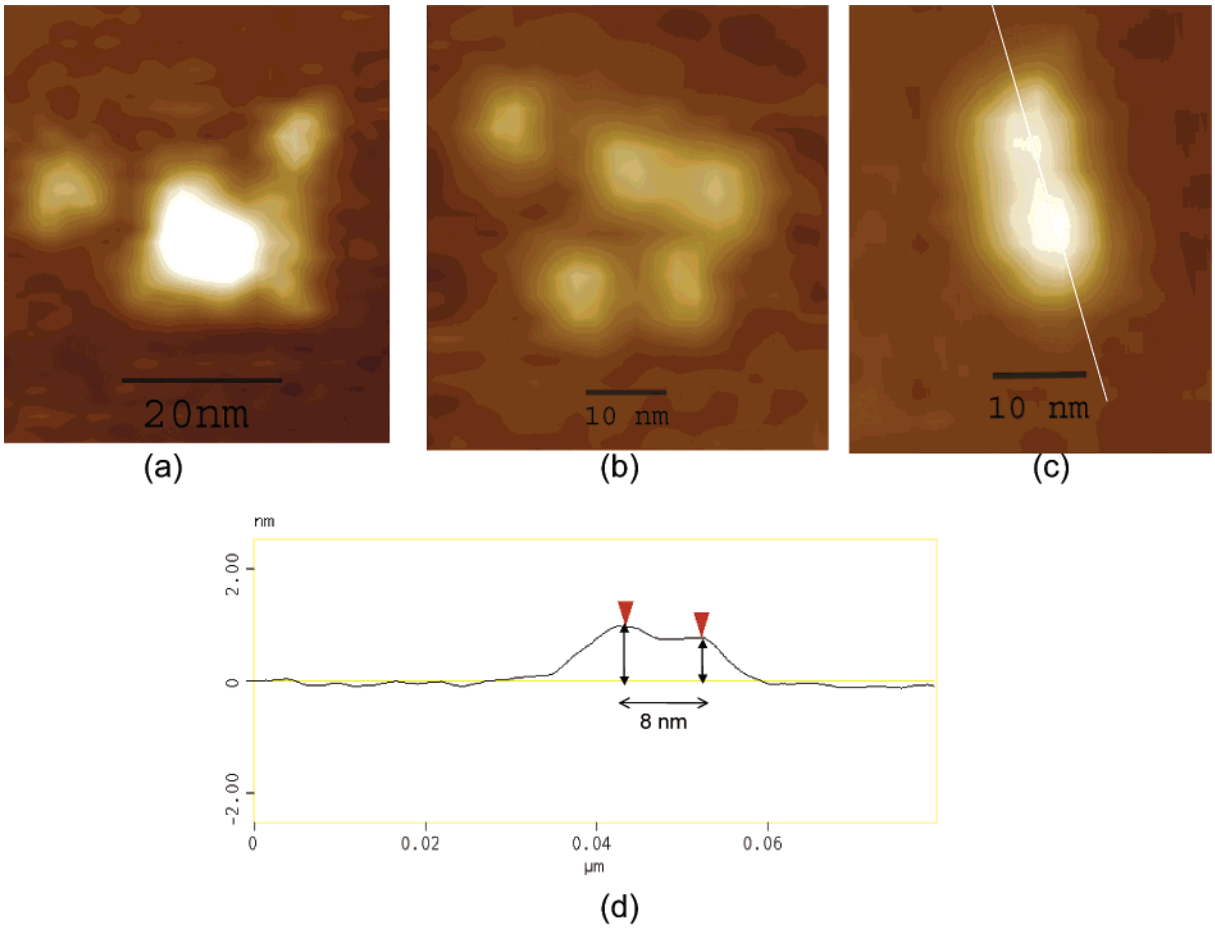

Figure 5. AFM sectional analysis of G7 and G5 dendrimer mixtures (particles C, D, and E of Figure 4). Although several G5 dendrimers appear to be aggregated almost as if in a cluster (a), others are randomly distributed (b), and all have inconsistent distances between the polymer molecules. Even an apparently linked structure found in the mixture (c) demonstrated a small distance (8−10 nm) between dendrimers when a sectional analysis of the image was performed (d).

the oligonucleotide to the dendrimer by EDC/imidazole chemistry and the removal of unreacted oligonucleotide from the conjugate with preparative agarose gel electrophoresis allowed us to generate an oligonucleotide−dendrimer conjugate in a reproducible and controlled manner.

Hybridization of the resulting single-stranded (ss) DNA-conjugated G7 and G5 dendrimers was carried out in an equimolar ratio to prevent cross linking and the formation of very large complexes. The reaction mixture in a hybridization buffer (10 mM Tris, 1 mM EDTA, 100 mM NaCl) was heated at 90 °C for 10 min and then allowed to cool to room temperature over 3 h. The modeled size and shape of the oligonucleotides G7−G5 PAMAM dendrimer self-assembly are schematically displayed in Figure 1, where a theoretical length of the oligonucleotide was calculated using 4.3 and 3.4 Å per base for single-stranded DNA and double-stranded DNA, respectively.[22] The diameter of an amine-terminated PAMAM dendrimer has been reported to be approximately 8 nm for G7 and 5 nm for G5.[23,24] However, the diameter of partially acetylated dendrimers was found to be only 5.0 nm for G7 and 4.7 nm for G5 from SEC analysis (Table 1). This is explained by a decrease in surface amine repulsion, which leads to a decrease in dendrimer size, related to the degree of acetylation.[14]

Dynamic light scattering (DLS) analysis allowed the measurement of the DNA-linked dendrimer's cluster size in solution (Figure 3). DLS measurements of the dendrimers, dendrimer−oligonucleotide conjugates, and DNA-linked dendrimer clusters were performed using an PSS/NICOMP 380 ZLS particle sizing system (Santa Barbara, CA) with a red-diode laser at 635 nm in a multiangle round cell. Number-weighted data from each sample at 90° was collected using a software calculation (CW 380, version 1.5) on the particle distribution after 20 min of running time. NICOMP size distribution analysis, recommended for broad or polydisperse samples, was used for data interpretation. The resulting hydrodynamic radii are derived from apparent diffusion coefficients using the Stokes−Einstein equation

$$D = \frac{kT}{6\pi\eta R_h}$$

where R_h is the hydrodynamic radius, η is the solvent viscosity (0.933 cp for water), k is Boltzmann's constant, and T the absolute temperature (296 K).[25]

Compared to the latex particle-size standards (20, 30, and 50 nm), the conjugates and their hybrid showed broad Gaussian distributions, suggesting the polydispersity of the

Table 2. Characteristics of Oligonucleotides Used in This Study

name	sequences[a]	base length	extinction coefficient ($M^{-1}\,cm^{-1}$)	calculated length (nm)[b]	M_w (g/mol)	T_m[c] (°C)
CON34	5′[P]GGCCATATAGGCCTTTT *GGCCTATATGGCCGGGGG3′*	34	317,632	14.6	10 553	74
SON34	5′[P]CCCCGGCCATATAGG*C CAAAAGGCCTATATGGCC*3′	34	325,499	14.6	10 429	74
CON50	5′[P]GGGGGGGTTTT*TTTTGG CCATATAGGCCTTTTGGCCTA TATGGCCTTTT*3′	50	521,172	21.5	15 535	75
SON50	5′[P]GGGGGGGGAAAAAAAA *GGCCATATAGGCCAAAAGGC CTATATGGCCAAAA*3′	50	617,647	21.5	15 679	75
CON66	5′[P]GGGGGGTTTTTTGGGG GGTTTTTTGGGG*TTTTGGCC ATATAGGCCTTTTGGCCTATA TGGCCTTTT*3′	66	600,758	28.4	20 836	77
SON66	5′[P]GGGGGGAAAAAAGGG GGGAAAAAAGGGG*AAAAGG CCATATAGGCCAAAAGGCCTA TATGGCCAAAA*3′	66	742,375	28.4	20 620	77

[a] Italicized letters indicate the region where the complementary base paring occurs. [b] Calculated from the literature, where the lengths of ssDNA and dsDNA in TE/NaCl are reported to be 4.3 and 3.4 Å per base, respectively.[16] [c] T_m indicates, by definition, the melting temperature of DNA at which the oligonucleotide is annealed to 50% of its exact complement and is calculated at the 50 mM NaCl concentration.

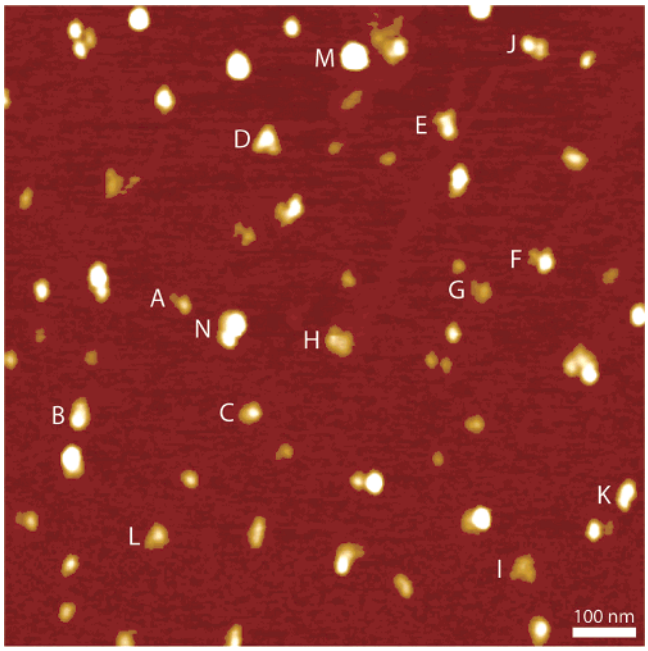

Figure 6. Representative AFM image of DNA-linked G7 and G5 PAMAM dendrimer clusters in air using partially complementary ssDNAs (cON50 and sON50) on mica (1 μm × 1 μm). The image analysis of 12 clusters marked as A to L is shown in Table 3. M and N are examples of large aggregates of the clusters.

Table 3. Image Analysis of Representative DNA-Linked G7 and G5 PAMAM Dendrimer Nanoclusters in Figure 3[a]

cluster	*h*1 (nm)	*h*2 (nm)	V^b (nm^3)	*d* (nm)
A	0.7	0.2	260	21
B	1.4	0.7	302	23
C	1.0	0.6	202	14
D	1.6	0.7	372	19
E	1.1	1.0	335	19
F	1.4	0.5	438	23
G	1.5	0.5	130	20
H	0.7	0.6	330	21
I	0.6	0.4	280	18
J	1.0	0.6	235	22
K	1.2	1.0	256	17
L	0.8	0.4	290	18
average	1.1 ± 0.3	0.6 ± 0.2	286 ± 80	21 ± 2

[a] *h*1: maximum height; *h*2: minimum height; *V*: total volume; *d*: interdendrimer distance. [b] Each volume measurement was within 10% of the standard deviation.

samples tested. Thus, the NICOMP number-weighted distribution analysis was used to obtain the particle-size distribution. The average diameter of the partially acetylated dendrimers was observed to be below 10 nm, which is the detection limit of our instrument. However, the DNA-linked dendrimer clusters showed a hydrodynamic diameter of 30 to 50 nm, which was much larger than the corresponding nonclustered dendrimer−oligonucleotide diameters that averaged 10 nm regardless of oligonucleotide length (Figure 3). Remarkably, the overall sizes of the hybrid of the dendrimer−oligonucleotide conjugates increased according to the length of the oligonucleotides and showed a stable size distribution during the measurement for 20 min. These results are in good agreement with the expected diameters of the dimer structure of dendrimers linked with the oligonucleotides.

We also used tapping-mode atomic force microscopy (AFM) analysis to prove our concept of the DNA-mediated self-assembly of the dendrimers. AFM measurements were performed on a Nanoscope IIIa Multimode scanning probe microscope from Digital Instruments (Veeco Metrology Group, Santa Barbara, CA). The tips were manufactured by Nanosensors (Wetzlar-Blankenfeld, Germany, distributed by

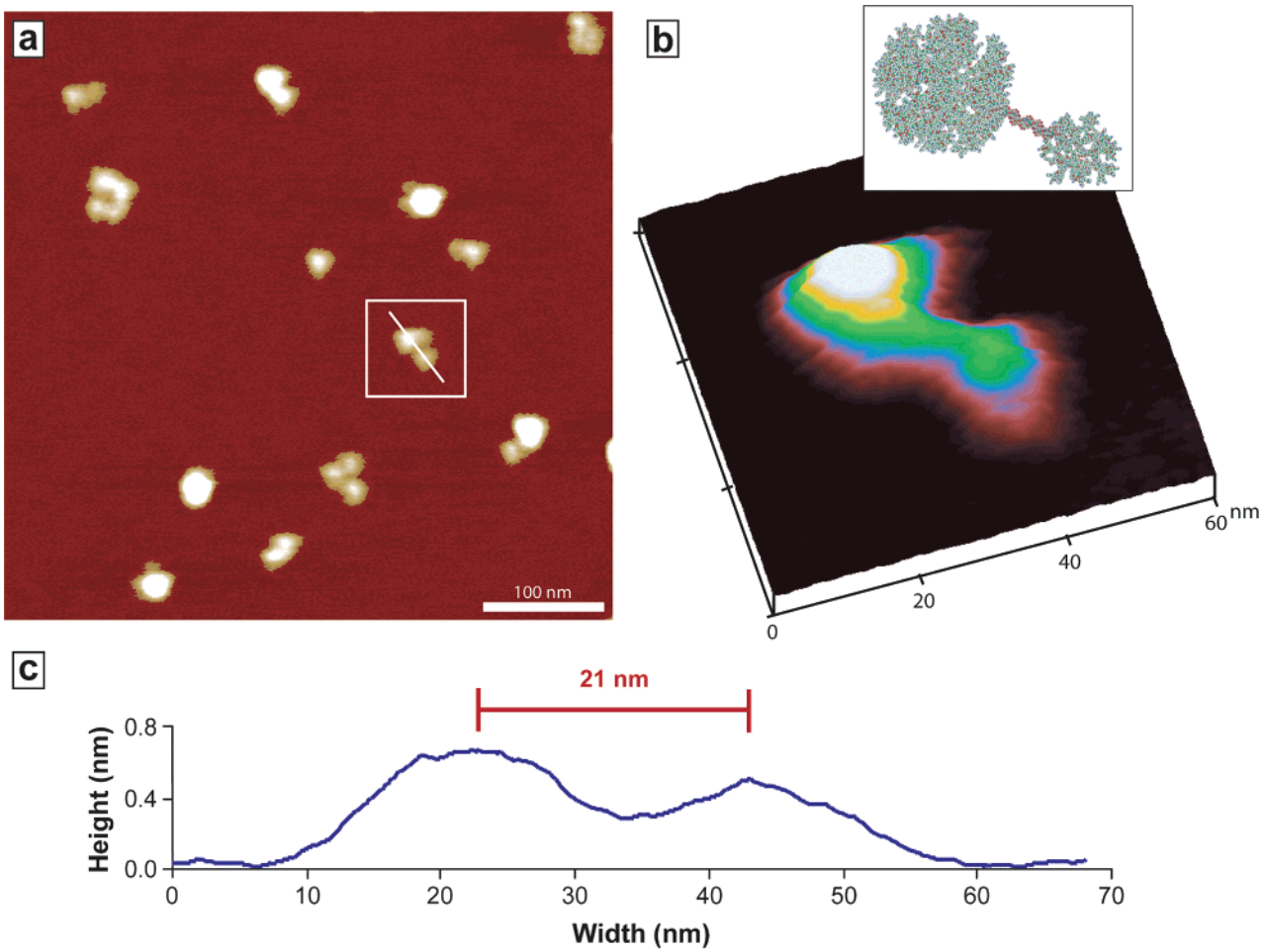

Figure 7. (a) Representative image of a DNA-linked G7−G5 dendrimer nanocluster on mica (500 nm × 500 nm), (b) 3D image of one single dimeric cluster boxed in (a), and (c) line-scan analysis of the cluster in (b). The interdendrimer distance was theoretically calculated to be 20 nm and observed to be 21 ± 2 nm on average.

Molecular Imaging, Phoenix, AZ) and had a NCH-W point probe that was 125 μm in length with a resonance frequency range of 297−378 kHz and a force constant range of 29−61 N/m. Image analysis was performed according to the numerical integration of each feature using the bearing analysis of the Nanoscope III software to yield accurate volume calculations. Theoretically, the volumes of G5 dendrimers are expected to be in the range of 40−60 nm^3, and the those of the G7 dendrimers, in the range of 160−230 nm^3 depending on the degree of acetylation.[26]

For comparison purposes, the equimolar mixture of the partially acetylated G7 and G5 PAMAM dendrimers at a concentration of 7 nM was imaged. The mixture of two differently sized dendrimers showed a random distribution (Figure 4; A and B) with no specific linkage between the dendrimers and aggregated on a mica substrate without consistent interdendrimer distances (Figure 4; C, D, and E). Sectional analysis also indicated that the few dendrimers in close proximity showed only a small distance of 8 nm between the two dendrimers. This suggested that the dendrimers are merely in physical contact with each other on the mica (Figure 5).

Figure 6 shows a representative example of AFM images of the DNA-linked dendrimer nanoclusters adsorbed to mica in a dry state. Some of the larger objects appeared to be aggregates of many individual dendrimers and/or dendrimer clusters. However, there are a number of smaller, dumbbell-shaped clusters whose dimensions are consistent with the ones expected for individual DNA-linked dendrimers. Table 3 summarized the AFM image analysis of 12 objects (A to L) regarding the maximum and minimum heights, total volume, and horizontal distance between the dendrimers. Some of the particles, such as M and N, have larger volumes, indicating that more than two dendrimers with a few oligonucleotides attached have assembled into a cluster. Remarkably, the average volume (286 ± 80 nm^3) of the 12 objects suggests assemblies of 2 or 3 dendrimers, which is close to that expected in a dimeric or trimeric dendrimer cluster. The 3D image of a dimeric single cluster in Figure 7 shows that the total volume is consistent with two oligonucleotide-linked G7 and G5 dendrimers, whereas the interdendrimer distance of approximately 20 nm consistently agrees with the length of the partially complimentary ON50 oligonucleotides pairs. Note that the very low aspect ratio of these topographical features helps to minimize tip convolution effects in the volume measurement.[27] A selection of representative PAMAM dendrimer clusters is also displayed in Figure 8, where the dimeric or trimeric dendrimer

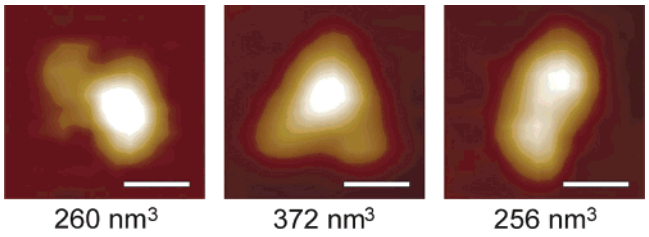

Figure 8. Representative nanoclusters in AFM images with their volumes and interdendrimer distances in good agreement with theoretical calculations of the dimeric or trimeric self-assembly of G7 and G5 PAMAM dendrimers via DNA. The numbers below the image indicate the total volume based on a numerical integration method. Bars indicate 20 nm.

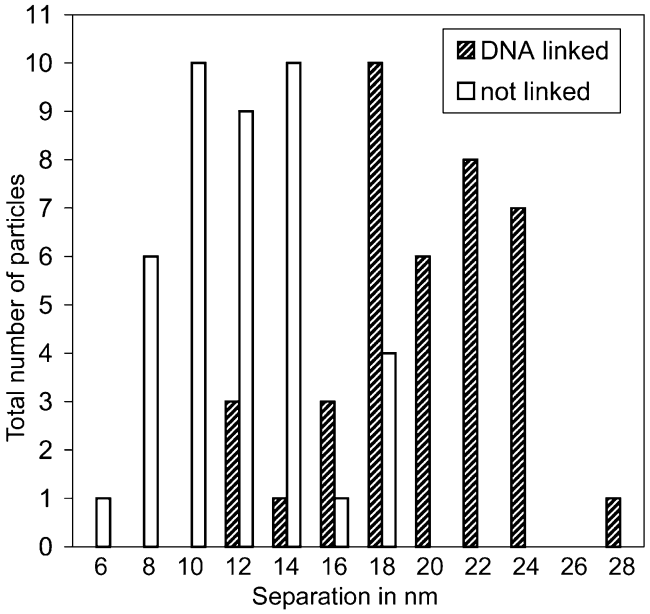

Figure 9. Comparison of the interdendrimer distance of the mixture of G7 and G5 and the DNA-linked G7 and G5 nanoclusters in the AFM images.

nanoclusters have a consistent interdendrimer distance and a total volume ranging from 200 to 400 nm^3. Despite the clumping and distortion of the complex morphology due to the drying of the samples on mica, the AFM images clearly demonstrate a variety of nanostructures consisting of the partially acetylated G7 and G5 dendrimers self-assembled by DNA hybridization, compared with the mixture of the dendrimers. Importantly, the statistical analysis of the DNA-linked nanoclusters in terms of the distance between the dendrimers in comparison with the mixture of the dendrimers provided significant evidence of the DNA-directed self-assembly of the dendrimers (Figure 9).

These initial results demonstrate that the design of simple and effective systems for DNA-linked dendrimers can be achieved. These unique structures have a number of advantages as supramolecular arrays, such as self-assembly without additional reactants and the possible assembly of specific dendrimer conjugates that have multiple functional groups attached to their surfaces.[28−30]

Acknowledgment. This project has been funded in whole or in part with federal funds from the National Cancer Institute, National Institutes of Health, under contract no. NO1-CO-27173. We are grateful to Timothy Sassanella for his design of the oligonucleotide sequence and helpful discussions. We also thank Jessica Hessler for her contribution to the AFM analysis of the dendrimer nanostructures.

Supporting Information Available: Detailed information on the preparation and characterization of the partially acetylated G7 and G5 PAMAM dendrimers. This material is available free of charge via the Internet at http://pubs.acs.org.

References

(1) Storhoff, J. J.; Mirkin, C. A. *Chem. Rev.* **1999**, *99*, 1849−1862.
(2) Tomalia, D. A.; Naylor, A. M.; Goddard, W. A. *Angew. Chem., Int. Ed. Engl.* **1990**, *29*, 138−175.
(3) Tomalia, D. A. *Adv. Mater.* **1994**, *6*, 529−539.
(4) Uppuluri, S.; Swanson, D. R.; Piehler, L. T.; Li, J.; Hagnauer, G. L.; Tomalia, D. A. *Adv. Mater.* **2000**, *12*, 796−800.
(5) Alivisatos, A. P.; Johnsson, K. P.; Peng, X. G.; Wilson, T. E.; Loweth, C. J.; Bruchez, M. P.; Schultz, P. G. *Nature* **1996**, *382*, 609−611.
(6) Mirkin, C. A.; Letsinger, R. L.; Mucic, R. C.; Storhoff, J. J. *Nature* **1996**, *382*, 607−609.
(7) Waybright, S. M.; Singleton, C. P.; Wachter, K.; Murphy, C. J.; Bunz, U. H. F. *J. Am. Chem. Soc.* **2001**, *123*, 1828−1833.
(8) Bielinska, A.; Kukowska-Latallo, J. F.; Johnson, J.; Tomalia, D. A.; Baker, J. R. *Nucleic Acids Res.* **1996**, *24*, 2176−2182.
(9) Kukowska-Latallo, J. F.; Bielinska, A. U.; Johnson, J.; Spindler, R.; Tomalia, D. A.; Baker, J. R. *Proc. Natl. Acad. Sci. U.S.A.* **1996**, *93*, 4897−4902.
(10) DeLong, R.; Stephenson, K.; Loftus, T.; Fisher, M.; Alahari, S.; Nolting, A.; Juliano, R. L. *J. Pharm. Sci.* **1997**, *86*, 762−764.
(11) Richardson, S. C. W.; Pattrick, N. G.; Man, Y. K. S.; Ferruti, P.; Duncan, R. *Biomacromolecules* **2001**, *2*, 1023−1028.
(12) Bell, S. A.; McLean, M. E.; Oh, S. K.; Tichy, S. E.; Zhang, W.; Corn, R. M.; Crooks, R. M.; Simanek, E. E. *Bioconjugate Chem.* **2003**, *14*, 488−493.
(13) Tomioka, N.; Takasu, D.; Takahashi, T.; Aida, T. *Angew. Chem., Int. Ed.* **1998**, *37*, 1531−1534.
(14) Majoros, I. J.; Keszler, B.; Woehler, S.; Bull, T.; Baker, J. R. *Macromolecules* **2003**, *36*, 5526−5529.
(15) Quintana, A.; Raczka, E.; Piehler, L.; Lee, I.; Myc, A.; Majoros, I.; Patri, A. K.; Thomas, T.; Mule, J.; Baker, J. R. *Pharm. Res.* **2002**, *19*, 1310−1316.
(16) Tomalia, D. A. *Macromol. Symp.* **1996**, *101*, 243−255.
(17) Chu, B. C. F. *Nucleic Acids Res.* **1983**, *11*, 6513−6529.
(18) Tung, C. H.; Stein, S. *Bioconjugate Chem.* **2000**, *11*, 605−618.
(19) Tomioka, N.; Takasu, D.; Takahashi, T.; Aida, T. *Angew. Chem., Int. Ed.* **1998**, *37*, 1531−1534.
(20) Bielinska, A. U.; KukowskaLatallo, J. F.; Baker, J. R. *Biochim. Biophys. Acta* **1997**, *1353*, 180−190.
(21) Ottaviani, M. F.; Furini, F.; Casini, A.; Turro, N. J.; Jockusch, S.; Tomalia, D. A.; Messori, L. *Macromolecules* **2000**, *33*, 7842−7851.
(22) Tinland, B.; Pluen, A.; Sturm, J.; Weill, G. *Macromolecules* **1997**, *30*, 5763−5765.
(23) Li, J.; Piehler, L. T.; Qin, D.; Baker, J. R.; Tomalia, D. A.; Meier, D. J. *Langmuir* **2000**, *16*, 5613−5616.
(24) Jackson, C. L.; Chanzy, H. D.; Booy, F. P.; Drake, B. J.; Tomalia, D. A.; Bauer, B. J.; Amis, E. J. *Macromolecules* **1998**, *31*, 6259−6265.
(25) Elizalde, O.; Leal, G. P.; Leiza, J. R. *Part. Part. Sys. Charact.* **2000**, *17*, 236−243.
(26) Betley, T. A.; Holl, M. M. B.; Orr, B. G.; Swanson, D. R.; Tomalia, D. A.; Baker, J. R. *Langmuir* **2001**, *17*, 2768−2773.
(27) Betley, T. A.; Hessler, J. A.; Mecke, A.; Holl, M. M. B.; Orr, B. G.; Uppuluri, S.; Tomalia, D. A.; Baker, J. R. *Langmuir* **2002**, *18*, 3127−3133.
(28) Quintana, A.; Raczka, E.; Piehler, L.; Lee, I.; Myc, A.; Majoros, I.; Patri, A. K.; Thomas, T.; Mule, J.; Baker, J. R. *Pharm. Res.* **2002**, *19*, 1310−1316.
(29) Esfand, R.; Tomalia, D. A. *Drug Discovery Today* **2001**, *6*, 427−436.
(30) Patri, A. K.; Majoros, I. J.; Baker, J. R. *Curr. Opin. Chem. Biol.* **2002**, *6*, 466−471.

NL0343497